frontiers | Frontiers in Marine Science

ORIGINAL RESEARCH
published: 24 June 2022
doi: 10.3389/fmars.2022.887240

Different Responses of Chlorophyll a to the Passage of the Tropical Storm Wipha (2019) in the Coastal Waters of the Northern Beibu Gulf

Ying Chen[1,2,3], *Chaoxing Ren*[4], *Yuting Feng*[1], *Haiyi Shi*[1,2,3], *Gang Pan*[2,5]*, *Mick Cooper*[5] *and Hui Zhao*[1,2,3]*

[1] College of Chemistry and Environmental Science, Guangdong Ocean University, Zhanjiang, China, [2] Research Center for Coastal Evironmental Protection and Ecological Remediation, Guangdong Ocean University, Zhanjiang, China, [3] Southern Marine Science and Engineering Guangdong Laboratory, Zhuhai, China, [4] Marine Environmental Monitoring Center of Guangxi, Beihai, China, [5] School of Animal, Rural and Environmental Sciences, Nottingham Trent University, Brackenhurst, Southwell, United Kingdom

OPEN ACCESS

Edited by:
Jie Xu,
University of Macau, China

Reviewed by:
Dilip Kumar Jha,
National Institute of Ocean Technology, India
Gabor Varbiro,
Hungarian Academy of Sciences, Hungary

***Correspondence:**
Hui Zhao
huizhao1978@163.com
Gang Pan
gang.pan@ntu.ac.uk

Specialty section:
This article was submitted to Marine Biogeochemistry, a section of the journal Frontiers in Marine Science

Received: *01 March 2022*
Accepted: *23 May 2022*
Published: *24 June 2022*

Citation:
Chen Y, Ren C, Feng Y, Shi H, Pan G, Cooper M and Zhao H (2022) Different Responses of Chlorophyll a to the Passage of the Tropical Storm Wipha (2019) in the Coastal Waters of the Northern Beib Gulf. Front. Mar. Sci. 9:887240. doi: 10.3389/fmars.2022.887240

Tropical storms (TS) are important drivers of short-term changes and affects the coastal and marine environment. Based on *in situ* observational data from four locations in the coastal area of the northern Beibu Gulf and satellite data, we analyzed the changes in temperature, salinity, and turbidity during the transit of TS "Wipha" in 2019 and assessed the environmental factors controlling chlorophyll a concenteation (Chl-*a*) increases in the coastal area. Our results showed that in the coastal area, the growth of phytoplankton after the TS was mainly controlled by the nutrient and light availability. The increased input of freshwater by TS, including direct inputs from rainfall and increased river discharge, reduced the salinity. The decrease in salinity may indicate an increased input of nutrient-rich freshwater at all four stations (nutrients input: S1>S2>S3>S4). Nutrient concentration at S1, S2, and S3 implied by salinity was high, but that at S4 was limited. The shorter recovery time of turbidity after TS indicated the faster improvement of light conditions in this area [recovery time: S4 (2 days)< S1 (3 days)< S3 (5 days)< S2 (10 days)]. The high turbidity associated with poor light penetration was an important factor limiting phytoplankton growth at station 2, with a slow recovery of the turbidity to pre-TS levels. The rapid recovery of the turbidity to the pre-TS levels at S1, S3, and S4 suggested good light conditions soon after the TS, and probably led to a significant increase in Chl-*a* after the TS ([Chl-*a*]: S1>S3>S4). The less of an increase of Chl-*a* at S4 was not only related to nutrient restriction but also related to weak mixing of the water column, while the least significant decrease in the SST at S4 implied that the enhancing mixing after TS was limited.

Keywords: Beibu Gulf, tropical storm, turbidity, sea surface temperature, chlorophyll a

INTRODUCTION

Variations in the concentration of chlorophyll a (Chl-*a*) are closely related to the environmental quality and are used to measure the spatial and temporal distribution of Chl-*a* (Zhao and Zhang, 2014). Chl-*a* is a key index in the measurement of phytoplankton biomass. It plays an important role in the marine atmospheric carbon cycle, energy conversion, and environmental monitoring. However, phytoplankton blooms also have a negative impact on aquaculture, fisheries, marine environment, and human health. Located in the northwestern South China Sea (SCS), the Beibu Gulf is a semi-enclosed bay shared by China and Vietnam (Lai et al., 2014), which is a shallow bay with a water depth of less than 50 m (**Figure 1B**). The summer water circulation in the Beibu Gulf is complex due to the combined effects of wind, heat flux, and river plumes (Gao et al., 2017). The summer circulation is cyclonic in the northern Beibu Gulf (Gao et al., 2017). Environmental problems are increasing in coastal areas worldwide as a result of rapid growth in the human population and economy. The coastal area of the northern Beibu Gulf is affected by a large amount of waste water from agriculture and domestic as well as industry (Kaiser et al., 2013), which has led to eutrophication and excess nutrients. High concentrations of dissolved inorganic nitrogen and phosphate are found in the northern Beibu Gulf (Lai et al., 2014). Some of the high pollution loads in the northern coastal areas are input from the Qinjiang, Maoling, and Nanliu rivers (**Figure 1B**) (Kaiser et al., 2014; Lai et al., 2014; Lao et al., 2019). These rivers provide abundant freshwater and nutrients to the coastal areas of the gulf, affecting the sea surface temperature (SST), salinity (SP), turbidity, and phytoplankton growth (Maren and Hoekstra, 2005; Maren, 2007).

The northwestern continental shelf of the SCS is a region intruded frequently by tropical cyclones from the SCS or the Northwest Pacific Ocean (Liu et al., 2011), with an average of nine to 14 tropical cyclones passing through every year (Chen et al., 2012). Based on comparisons of two typhoons with different moving speeds and maximum sustained wind speeds, Zhao et al. (2008) found that the wind stress of fast-moving strong typhoons has a limited impact on the upper ocean due to their short forcing time, and the typhoon with a slower moving speed can cause stronger entrainment and greater time-integration displacement vertically, inducing one stronger phytoplankton bloom. Typhoon "Damrey" caused two phytoplankton blooms in the northern SCS through upwelling and vertical mixing (Zheng and Tang, 2007). Based on a coupled atmosphere-ocean model in the SCS, Wu et al. (2019) found that the heat carried by the vaporization of the sea surface was one also of the important factors for the decrease of sea temperature under the influence of a typhoon. Storm events can alter productivity patterns by flushing or mixing "new" nutrients into the water column (Wetz and Paerl, 2008). In turn, these nutrients may cause massive phytoplankton blooms and compositional changes in the phytoplankton community (Paerl et al., 2006; Miller and Harding, 2007). The variations of oceanic responses induced by a tropical cyclone with different intensities are different. A previous study showed that the upwelling velocity induced by the cyclonic stress curl was roughly proportional to tropical cyclone intensity, which implied that tropical cyclone intensity had an important impact on the uplift of nutrients and the growth of phytoplankton (Zhao et al., 2013). Zhao et al. (2017) also proved that the Chl-*a* increase was shown to be highly correlated with the tropical cyclone intensity. The weak tropical cyclones (tropical storm) would also exert significant influence on phytoplankton in the nearshore region, because the relatively shallower nutricline, depth, and thermocline in the nearshore region before the storm are favorable for uplift of nutrients (Zhao et al., 2017). These weather events can promote the proliferation of marine phytoplankton, thereby increasing the primary productivity of the ocean (Foltz et al., 2015; Liu et al., 2019), and may have important effects on marine biogeochemical processes (Shang et al., 2008).

There have been a number of studies on the impact of strong tropical cyclones on phytoplankton and primary productivity in open sea areas, such as the western Pacific and far from the continental shelf of the SCS (Price, 1981; Lin et al., 2003; Babin

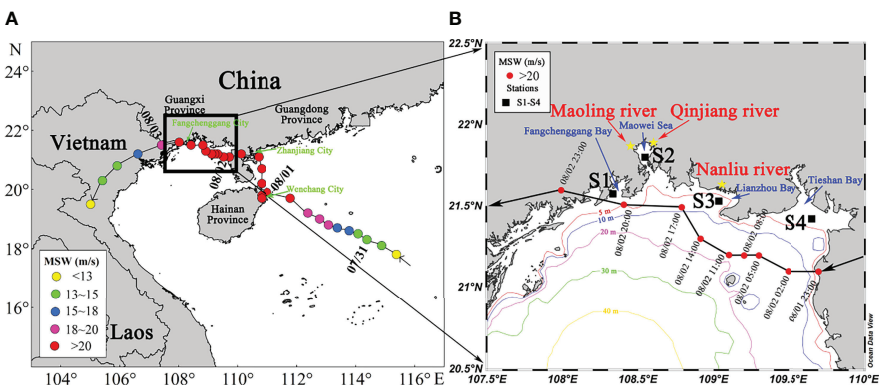

FIGURE 1 | **(A)** Track and intensity of TS Wipha in the northwestern SCS. **(B)** Depth map of the northern Beibu Gulf in the study area (20.5° N-22.5° N, 117.5° E-110° E). Black squares are the observational stations (S1-S4). Yellow stars mark the river estuaries. MSW: maximum sustained wind speed. Dates are given as mm/dd.

et al., 2004; Zhao et al., 2008; Lin, 2012; Zhao et al., 2017). Wind-induced upwelling and the mixing of "new" nutrients may produce phytoplankton blooms and increase the primary productivity in open ocean areas (Price, 1981; Chang et al., 1996; Chen et al., 2003; McKinnon et al., 2003; Babin et al., 2004). The response of continental shelf seas to tropical cyclones may be different from that of open ocean areas as a result of the local environmental conditions (Xie et al., 2017). The increase in phytoplankton in the continental shelf region is regulated not only by the near-inertial oscillations induced by the uplift of nutrients, but also by the advection of nutrients, associated with enhanced runoff (Zheng and Tang, 2007; Zhao et al., 2017). But the effects of tropical cyclones on phytoplankton growth in coastal areas, especially estuaries, require further study. The influence of tropical cyclones on the Chl-*a* concentration at the sea surface is significantly different in different areas. We need to conduct long-term observations to accurately and comprehensively understand how tropical cyclones affect Chl-*a* concentration in coastal regions.

Wipha was the seventh tropical storm (TS) of 2019 and occurred from July 30 to August 3. The TS originated in the northern SCS (at about 115.4° E, 17.8° N) and had a maximum sustained wind speed (MSW) of about 23 $m{\cdot}s^{-1}$ (**Figure 1**). The storm initially moved gradually northwest and intensified continuously. The TS first made landfall in Wenchang City, Hainan Province, China on August 1, 2019. It then continued to move north at a steady wind speed (about 23 $m{\cdot}s^{-1}$), made landfall again at Zhanjiang, Guangdong, China, and then moved westward. After passing over the coast of the northern Beibu Gulf, the TS subsequently made a third landfall at Fangchenggang, Guangxi, China. After landfall, the TS rapidly weakened and moved southwest through Vietnam.

We used data from *in situ* observations and satellite to analyze the spatial variation of the increase in the concentration of Chl-*a* caused by the passage of TS Wipha. Different responses of Chl-*a* concentration at four stations to the TS were further investigated in the coastal waters of the north Beibu Gulf. Based on the comprehensive analysis of the relationship between Chl-*a* concentration and environmental factors, the possible mechanism causing different responses of phytoplankton Chl-*a* after the TS passage. The study is helpful to better understand the effect of the environmental changes caused by TS on the increase of Chl-*a* in coastal regions.

MATERIALS AND METHODS

Satellite Products

The TS data are available from the best-track typhoon dataset from Typhoon Online (www.typhoon.org.cn) (Ying et al., 2014; Lu et al., 2021), which includes the location and intensity of tropical cyclones in the northwest Pacific Ocean including the SCS every 3 to 6 h since 1949. The data include the MSW and the longitude/latitude of the center of the TS every 3 h.

We used Advanced Scatterometer (ASCAT) 6 h sea surface wind (SSW) data provided by the Remote Sensing System (www.remss.com/) at a spatial resolution of (0.25°×0.25°). We obtained daily precipitation data from the Tropical Rainfall Measuring Mission (TRMM) of the National Aeronautics and Space Administration (NASA) (https://gpm.nasa.gov/data) at a spatial resolution of 0.10°.

The data of photosynthetically active radiation (PAR) derived from four different sensors of Sea WiFS, MODIS, MERIS, and VIIRS with GSM Model (Maritorena and Siegel, 2005; Maritorena et al., 2010) are generated from GlobColour database provided by HERMES. The merged daily products of PAR with a spatial resolution of 0.04°× 0.04° are obtained for the period from July 26 to August 16.

In Situ Observations

Four buoys equipped with water quality sensors were deployed in the northern coastal areas of the Beibu Gulf from July 26 to August 16, 2019 (**Figure 1**), respectively at the stations of S1-S4. The Chl-*a* concentration (i.e., fluorescence), temperature, salinity, and turbidity were continuously measured at a depth of 0.5 m below the sea surface using a YSI 6600V2 multiparameter water quality instrument (YSI Inc., Yellow Springs, USA). The dissolved inorganic nitrogen (DIN) was measured at S3 using a Systea nutrient probe analyzer (NPA; Systea S.p.A., Anagni, Italy). The above data were sampled every 30 min. After the observations were complete, the missing or invalid data were linearly interpolated to obtain a complete time series.

In situ Chl-*a* concentration derived from YSI 6600V2 multi-parameter water quality instrument (YSI-derived Chl-*a*) was measured every 30 min and first processed into daily Chl-*a* through 24-hr average (i.e., 0:00-24:00). The sum of Chl-*a* for 7 days (Chl-$a_{(sum)}$) was calculated:

$$Chl - a_{(sum)} = \sum_{i=1}^{n} Chl - a_{(i)}$$

where the Chl-$a_{(sum)}$ was the sum of Chl-*a* concentration for 7 days ($mg{\cdot}m^{-3}$) and n was the number of days in a week (n=7).

All the above-mentioned data analysis methods were performed in the software packages Origin, Ocean Data View, ArcGIS, and MATLAB.

RESULTS

Distribution of Temperature and Precipitation Before and After TS

The *in situ* observational data showed that the SST in the study region was relatively uniform high before the TS (**Figure 2A**). There was a lower SST patch near S3 during the TS (**Figure 2A**). One week after TS, there was a low nearshore SST and a high offshore in the study region. The SST increased slightly at S3 and S4, and continued to reduce at S1 and S2 1 week after TS. The SST recovered to roughly to the pre-TS SST (about 31°C-32°C) (**Figure 2A**) roughly 2 weeks later. Precipitation in the study region was significantly increased (>100 $mm{\cdot}day^{-1}$) during the TS (**Figure 2B**), which may have increased the input of

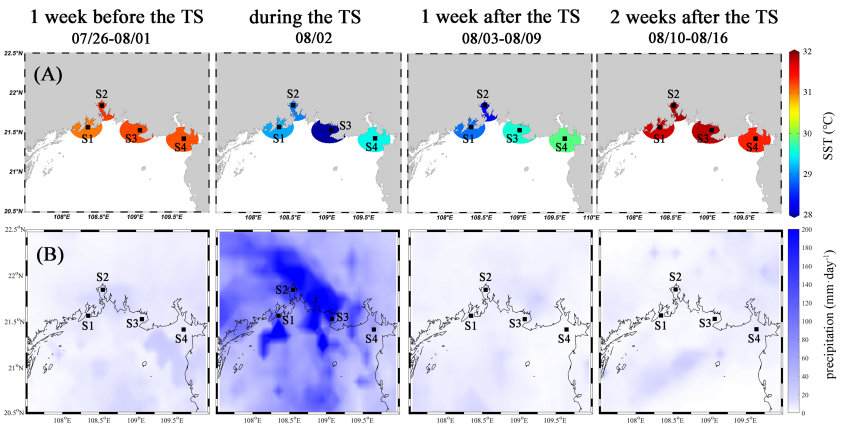

FIGURE 2 | **(A)** *In situ* SST data and **(B)** precipitation for four time periods (1 week before TS, during the TS, 1 week after TS, and 2 weeks after TS) in the northern Beibu Gulf.

freshwater, leading possibly to changes in the SST, salinity, and turbidity.

Physicochemical Parameters Before and After TS

The TS moved into the study region on August 1, 21:00, and left the study region on August 3, 02:00 (**Figure 1**). The SSW time series based on the regional average for the study region (20.5-22.5° N, 107.5-110.0° E) (**Figure 3**) showed that the SSW was < 6.0 $m{\cdot}s^{-1}$ from July 26 to July 30, with a maximum SSW of about 11.5 $m{\cdot}s^{-1}$ on August 1. The SSW quickly decreased after the TS had transited (**Figure 3**).

The SST at the four stations decreased significantly, with a maximum reduction of 2-4°C 1-2 days after the passage of the TS on August 3-4 (**Figure 4A**). The decrease in the SST (< 30°C) lasted for about 6 days. The SST increased slowly and only returned to the pre-TS level on August 11. The smaller standard deviation for the four stations indicated a concentrated distribution of the SST data (**Table 1**), which meant less SST variation at S4.

The time series of the salinity (**Figure 4B**) showed that the salinity of each station began to decrease after the TS had passed. S1 located in the landfall area of the TS was seriously affected by rainfall, and the salinity decreased by 13.5 1 day later. The salinity at S3, which was affected only by the River Nanliu, decreased by about 6.5 after the passage of TS. A low salinity appeared at S2 at the intersection of two rivers, which decreased by 8.5 2 days after the TS had passed. There was only a small, slow decrease in salinity at S4. The salinity decreased significantly at S1 and S2, resulting in large variations in their standard deviations (especially S2) (**Table 1**).

Although S1 was located in the landfall region of the TS, the maximum turbidity here after the TS (**Figure 4C**) was lower than that at S2 and S3 and recovered to the pre-TS levels only within 3 days. The turbidity of S2 was as high as 190 NTU on August 4, about nine times the pre-TS values (**Figure 4C**), which may be related to the greater influence of increasing estuarine runoff from the Maoling and Qinjiang rivers. It took 10 days for the turbidity of S2 to recover to pre-TS levels (**Figure 4C**). Similarly, the maximum turbidity of S3, which was

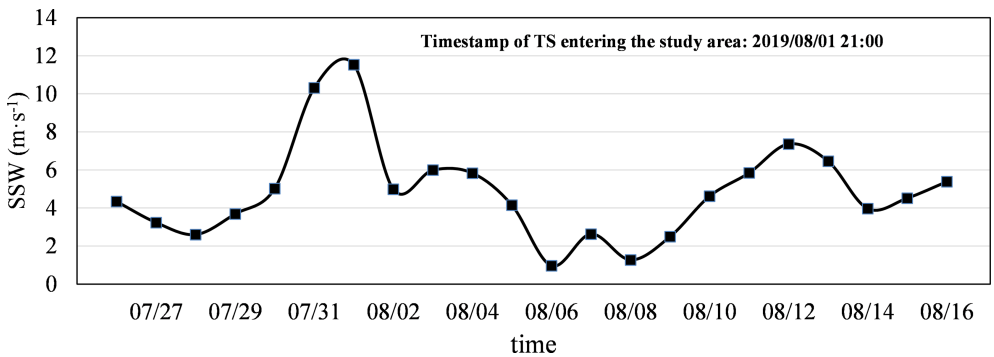

FIGURE 3 | Time series of SSW from July 26 to August 16, 2019, based on the regional average for the study region (20.5° N-22.5° N, 107.5° E-110° E).

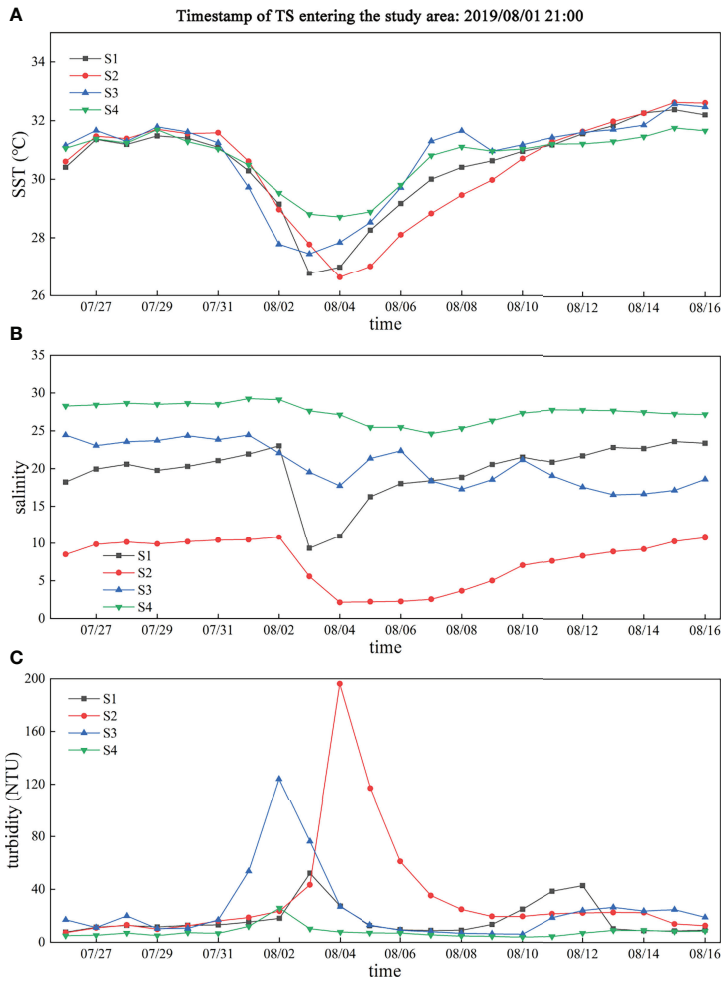

FIGURE 4 | Time series of **(A)** SST, **(B)** salinity, and **(C)** turbidity from July 26 to August 16, 2019.

affected also by one river (i.e., Nanliu River), reached up to 120 NTU (about six times the pre-TS values) (**Figure 4C**). The turbidity of S3 recovered to pre-TS levels within 5 days, faster than that of S2 (**Figure 4C**). Due to the offshore location of S4, a weaker increase in turbidity was recorded with the low maximum value of 25.8 NTU during the TS (i.e., about two to three times the pre-TS values), and quickly recovered to pre-TS levels within 2 days (**Figure 4C**). Tabulated data illustrated that S2 and S3 had high turbidity and large amplitude, while relatively lower for S1 and S4 (**Table 1**).

Ch-*a* Before and After TS

Our *in situ* data showed that the Chl-*a* concentration increased significantly in 1 to 2 weeks after the TS at all the stations except S2 (**Figure 5**). There was no obvious change in the Chl-$a_{(sum)}$ at S2 before and after the TS (**Figure 5A**). One week after the TS, there was a significant increase in the Chl-$a_{(sum)}$ concentration of about 60% (26.34 mg·m^{-3}) at S1, 68% (25.62 mg·m^{-3}) at S3, and 69% (14.86 mg·m^{-3}) at S4; the changes were smaller at S2 (**Figure 5A**). Two weeks after TS, the Chl-$a_{(sum)}$ concentration at S3 and S4 had decreased to roughly the levels 1 week before the

TABLE 1 | Daily average Chl-*a*, SST, salinity, and turbidity at four stations.

Stations	Chl-*a* (mg·m^{-3})	SST (°C)	Salinity (SP)	Turbidity (NTU)
S1	10.49 ± 11.08	30.50 ± 1.53	19.68 ± 3.53	17.28 ± 12.09
S2	4.43 ± 0.62	30.40 ± 1.76	7.57 ± 3.11	33.88 ± 42.26
S3	6.93 ± 3.03	30.75 ± 1.50	20.48 ± 2.84	25.19 ± 26.82
S4	3.84 ± 2.19	30.74 ± 0.93	27.43 ± 1.26	7.83 ± 4.41

Data presented as mean ± standard deviation; N = 22.

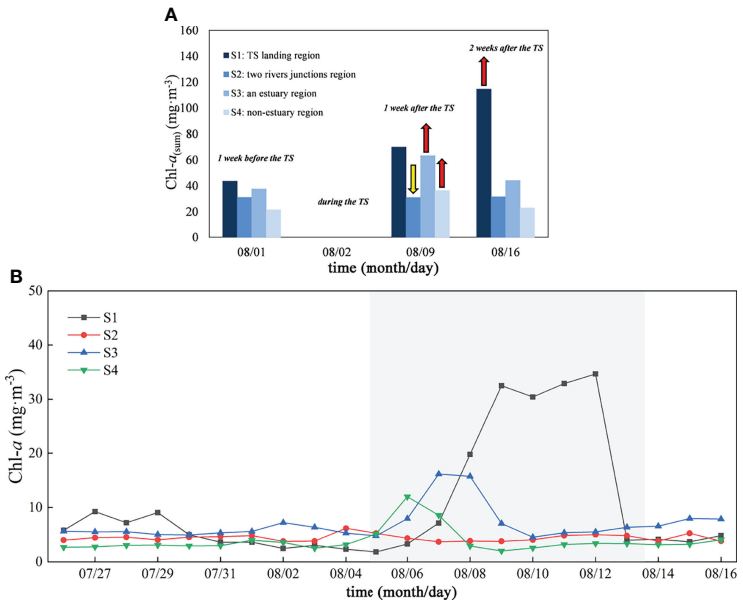

FIGURE 5 | **(A)** The sum of Chl-*a* concentration for 7 days for three time periods [1 week before TS (i.e., July 27- August 1), 1 week after TS (i.e., August 3- August 9), 2 weeks after TS, (i.e., August 10- August 16)] at S1-S4. Red arrows represent an increase in the Chl-$a_{(sum)}$; yellow arrows represent a decrease in the Chl-$a_{(sum)}$. **(B)** Chl-*a* time series of S1-S4. Gray shading indicates the process from an increase to a decrease in Chl-*a* at S1, S3, and S4.

TS (**Figure 5A**). At S1, the Chl-$a_{(sum)}$ concentration 2 weeks after the TS was about two times that 1 week before the TS (**Figure 5A**). The time series (**Figure 5B**) shows that the average Chl-*a* concentration began to increase about 3 days after the TS had transited, reaching > 10 mg·m^{-3} at S1, S3, and S4, especially highest at S1. The larger standard deviations of Chl-*a* concentration at S1, S3, and S4 indicate that the Chl-*a* concentration at the stations was more variable compared with S2 (**Table 1**).

Correlation Analysis of DIN and Salinity

Salinity was measured at all stations, while nutrient concentration (i.e., DIN) was measured only at S3. A simple correlation analysis between DIN and salinity at S3 was made to assess the possibility of changes in nutrient concentration at all stations estimated by salinity values, to a certain degree. The scatter graph (**Figure 6**) for DIN and salinity exhibited a sensible trend. A correlation analysis indicated that DIN was significantly negatively correlated with salinity ($R^2 = 0.7528$, $p < 0.01$) (**Figure 6**).

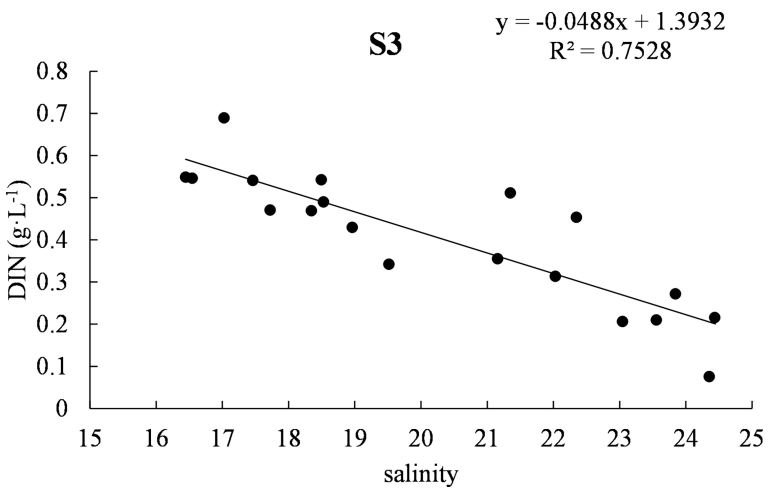

FIGURE 6 | Scatter diagrams of the salinity and DIN at S3 from July 26 to August 16, 2019.

DISCUSSION

Effects of the TS on Chl-*a* Concentration

Monitoring of Chl-*a* by means of traditional *in-situ* sampling has been difficult to be carried out under extreme weather events such as tropical storms. *In situ* fluorescence measurements can realize daily monitoring, hourly monitoring, and even continuous monitoring, which greatly improves the integrity and timeliness of monitoring data and helps to grasp the overall situation of the water body. Moreover, Chen and Zhao (2021) found the good relationship ($R^2 = 0.7407$, $p<0.01$) existed between Chl-*a* measured in the lab and YSI-derived Chl-*a* in coastal regions of the northwestern South China Sea, indicating that YSI-derived fluorescence can be used to estimate Chl-*a*.

There were significant changes in the SST, salinity, and turbidity (**Figure 4**) in the study region as a result of mixing following the passage of the TS. These changes will inevitably affect the growth of phytoplankton in the water column and, in turn, the Chl-*a* concentration. After the TS passage, the overall Chl-*a* concentration at S1, S3, and S4 showed an increasing trend (**Figure 5B**), roughly consistent with earlier studies (Wetz and Paerl, 2008; Zhao et al., 2017; Liu et al., 2020).

A negative correlation between total nitrogen/total phosphorus and salinity was generally assumed in coastal regions (Lane et al., 2002; Schaeffer et al., 2012). Moreover, our study confirmed also that the high correlation ($R^2 = 0.7528$, $p < 0.01$) was presented between DIN and salinity at S3, suggesting that the salinity can be used to imply changes in nutrients level (**Figure 6**) in the study. From the time series of salinity (**Figure 4B**), we knew that the nutrients at S1, S2, and S3 were full, but limited at S4. The salinity of S1, located in the landfall region of the TS (**Figure 1B**) and near the coast, decreased significantly by 13.5 in 1 day during the TS (**Figure 4B**), implying large amounts of nutrient-rich water input. The rapid (3 days) recovery in the turbidity to pre-TS levels resulted in good light conditions at S1 (**Figure 4B**), providing the conditions required for phytoplankton growth. Therefore, the two favorable conditions of the significant increase of nutrients and rapidly reduced turbidity after TS caused probably greater increase of Chl-*a* concentration and longer lasting time of high Chl-*a* concentration at S1 than those at S2, S3, and S4 (**Figure 5B**) after the passage of the TS.

S2 was located at the junction of two rivers (**Figure 1B**). The lowest salinity observed at S2 during the observational period suggested that there were large amounts of nutrient-rich freshwater input and nutrients were always available during the whole period before and after the TS (**Figure 4B**). However, the highest turbidity and slowest recovery time (10 days) limited the amount of light available at S2. There was no obvious increase in Chl-*a* concentration (**Figure 5**) despite the nutrient-rich freshwater.

S3 was located in the Lianzhou Bay and was affected by the inputs from the Nanliu River (**Figure 1B**). The salinity started to decrease on August 1 and this decrease lasted for 3 days (**Figure 4B**), probably suggesting a continuous supply of nutrients. With the high turbidity restoring rapidly (within 4 days) to low turbidity after TS (**Figure 4B**), the phytoplankton grew in large numbers, resulting in an increase in Chl-*a* concentration.

S4 was located offshore with less influence of nutrient-rich freshwater input from rivers (**Figure 1**). Therefore, the turbidity was lowest and the turbidity recovery time (2 days) was most rapidly at S4 (**Figure 4C**), reflecting the high availability of light in the region. The salinity at S4 was always the highest among the four stations and the decrease in salinity at S4 was less significant compared with other stations even during the passage of the TS. These suggested less of an increase of nutrient-rich freshwater at S4 after the TS and the supply of nutrients at S4 may still be the key to limiting the growth of phytoplankton. The temperature decrease (**Figure 4A**) under the influence of TS was the least significant at S4, which meant finite enhancing mixing implied after TS. The above conditions would have caused the increase in Chl-*a* concentration at S4 to not be the most significant (**Figure 5**).

Mechanism for the Formation of Nearshore Phytoplankton Blooms After TS

Previous research using remote sensing data had shown that the heavy rainfall caused by tropical cyclones increases generally the runoff from rivers in nearshore regions. This can lead to the transport of large amounts of nutrients, colored dissolved organic matter, and suspended sediments to coastal areas, contributing to the increase in Chl-*a* concentration (Chen et al., 2003; Zhao et al., 2009; Zhao et al., 2013). A fundamental limitation of remote sensing data is the inability to produce nearshore reliable measurements. Due to this limitation, our understanding of the response of Chl-*a* concentration in coastal areas to the passage of a TS is incomplete and needs to rely on the availability of *in situ* data. In our study, the results of *in situ* data showed that the growth of phytoplankton after the TS was not only affected by the nutrients brought by the increase of runoff but also related to the turbidity associated with light penetration.

Turbidity was negatively correlated with PAR ($R^2 = 0.2284$, $p<0.01$) (**Figure 7**) in our study, which meant that the greater the turbidity is roughly coincided with the lower the PAR in the study. Dou et al. (2019) also found that the light attenuation coefficient decreases when the water transparency increases. While turbidity was an important restrictive factor affecting the transparency of water, which can be verified by the logarithmic fitting equation based on the relationship between suspended solids and transparency (Zhang et al., 2003). Therefore, in our study, the rapid recovery of the turbidity after TS would mean more favorable light conditions, and vice versa, the slow recovery of the turbidity would limit light. With the decrease of turbidity (increase of transparency), PAR increased, resulting in the increase of phytoplankton photosynthesis and higher Chl-*a* concentration. The recovering time of turbidity to pre-TS levels was 3 days at S1, 10 days at S2, 5 days at S3, and 2 days at S4 (recovery time: S2>S3>S1>S4) (**Figure 4B**), respectively, suggesting the favorable light conditions soon after TS at S1, S3, and S4, as well as the bad light conditions at S2. According to the conditions of salinity (**Figure 4B**), nutrients were always available during the whole period at S1, S2, and S3, but limited at S4 (nutrients input: S1>S2>S3>S4). The intensity of the

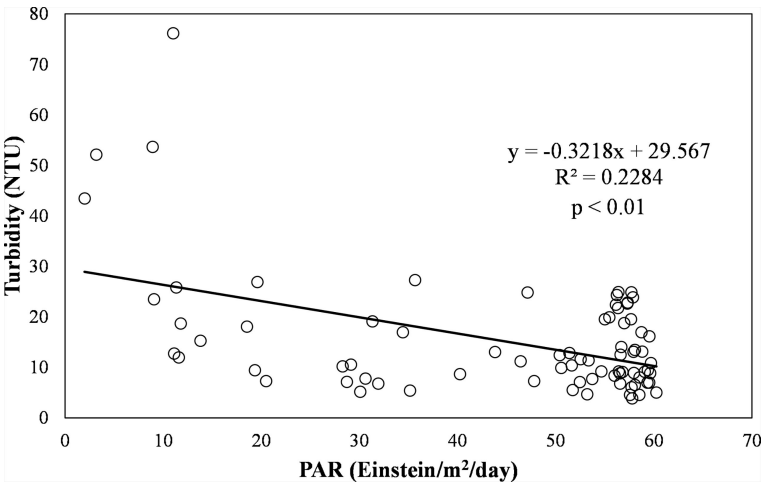

FIGURE 7 | The relationship between turbidity and PAR (R^2 = 0.2284, p<0.01) from July 26 to August 16.

phytoplankton blooms was the strongest at S1, followed by S3, then S4 (Chl-*a*: S1>S3>S4); the increase in Chl-*a* concentration was less significant at S2 (**Figure 5**). These may imply that nutrients had a more important role in the growth of phytoplankton at S1, S3, and S4 along with the favorable light conditions suggested by the turbidity rapidly recovering to pre-TS levels. Therefore, the most signifcant increase of nutrients along with favorable light conditions had probably induced the highest increase of Chl-*a* concentration at S1 after TS (**Figure 5**). Hagy et al. (2006) also reported that the input of freshwater from Hurricane Ivan led to one similar increase in the biomass of phytoplankton for several weeks in Pensacola Bay after the event.

In turbid coastal environments, light availability is usually the main driver of phytoplankton growth (Grobbelaar, 1990; Alpine and Cloern, 1992; Cloern, 1996; Kocum et al., 2002). The slow recovery of turbidity to pre-TS levels at S2 and the highest turbidity after TS suggested that the unfavorable light conditions into the water column, which was an important elementfor about 10 days after TS. Heavy rainfall during the TS (**Figure 2B**) led probably to large amounts of suspended particulate matter in the input from the Maoling and Qinjiang rivers, which may have reduced the transparency of the water at S2. Ma and Zhao (2021) have also found that, under normal circumstances, the Chl-*a* concentration in the nutrient-rich Pearl River estuary is low as a result of the high turbidity. Hence, the lack of available light limited the growth of phytoplankton in the water column at S2, although there were large amounts of nutrient-rich freshwater input implied by the salinity decreasing after TS. Moreover, the strong dilution from tropical rainfall during the storm and the mixing effects of the river input with high suspended matter limited also the accumulation of phytoplankton (Song et al., 2011), leading to a similar pattern of Chl-*a* concentration at S2 (**Figure 5**) before and after the TS. In other words, the input from rivers can change the hydrodynamic conditions to be unsuitable for phytoplankton growth, meaning that it took longer for levels to recover to those before the TS. Fu et al. (2009) showed that Chl-*a* concentration near the Pearl River estuary decreased by about 35% as a result of the high content of suspended matter after the passage of a typhoon. In these examples, light associated with the turbidity was the most important factor for the increase in Chl-*a* concentration at S2 under the conditions of sufficient nutrients, but a lack of light to promote phytoplankton growth.

A previous study indicated that the most significant response of the ocean to the TS was a decrease in the sea temperature (Yang and Tang, 2010). The data collected for this research indicated that the whole study area had cooled down after the passage of the TS (**Figure 2A**). The decrease in the SST (< 30 °C) caused by the TS lasted for about 6 days, but the level of the decrease in the SST was different at all four stations (**Figure 4A**). The decrease in temperature indicated the degree of mixing of the water column. The mixing induced by the TS forced the redistribution of surface stratification, which caused the decrease of SST and entrainment of nutrients into the upper layer of oceans (Wang et al., 1998; Shao et al., 2015). The cooling of S1 by about 4.3°C and S2 by about 5.0°C (**Figure 4A**), and the decrease in the SST lasted for 1 week, which meant that they were fully mixed. During the TS, on August 2, although the cooling of S3 was the fastest, its temperature quickly recovered 1 week later (**Figure 2A**). In contrast, the degree of mixing of S3 was not as significant as that of S1 and S2. S4 had slow cooling and fast recovery, and the mixing of this station was weak. The less of an increase of Chl-*a* concentration at S4 may be related to weak mixing of water column, to a certain degree.

CONCLUSIONS

We investigated the different responses of Chl-*a* concentration at four stations to the transit of one TS in a coastal region of north Beibu Gulf, the South China Sea, when TS Wipha moved over. The nutrient level and light availability were the two main driving factors regulating phytoplankton growth during the

study period. The better light conditions and richer nutrient concentration at S1 and S3 soon after the TS were more suitable for phytoplankton growth, shown as higher Chl-*a* concentration after TS. The most significant increase of nutrients along with favorable light conditions after TS caused the highest increase of Chl-*a* at S1. Whereas phytoplankton growth was limited by nutrients at S4 and light at S2, leading to less of an increase of Chl-*a* concentration at the above stations, especially at S2 with the highest turbidity. The increase in phytoplankton at S4 may also be related to the weak mixing of the water column during the TS. The growth of phytoplankton in the nearshore areas was therefore affected not only by the nutrients available but also by the other environmental factors, especially the turbidity.

DATA AVAILABILITY STATEMENT

The original contributions presented in the study are included in the article/supplementary material. Further inquiries can be directed to the corresponding authors.

AUTHOR CONTRIBUTIONS

YC and HZ conceived the idea presented here. YC, CR, HS, and HZ performed the analysis of the manuscript. YC processed the data and drafted the manuscript. YC and YF designed the figures. HZ was involved in planning and supervised the funding of this study. GP and MC revised the manuscript. CR was in charge of the field work (deployed the buoys and calibrated the sensors). All authors listed made a substantial, direct, and intellectual contribution to the study and approved it for publication.

FUNDING

The present research was supported by the National Natural Science Foundation of China (No. 42076162), Postgraduate Education Innovation Project of Guangdong Ocean University (202145), and project supported by Innovation Group Project of Southern Marine Science and Engineering Guangdong Laboratory (Zhuhai) (No. 311020004).

ACKNOWLEDGMENTS

We are grateful to Typhoon Online (www.typhoon.org.cn) for providing the tropical storm data, the Remote Sensing System (http://www.remss.com/) for providing the sea surface wind data, the National Aeronautics and Space Administration (https://gpm.nasa.gov/data) for providing the precipitation data.

REFERENCES

Alpine, A. A., and Cloern, J. E. (1992). Trophic Interactions and Direct Physical Effects Control Phytoplankton Biomass and Production in an Estuary. *Limnol. Oceanogr.* 37, 946–955. doi: 10.4319/lo.1992.37.5.0946

Babin, S. M., Carton, J. A., Dickey, T. D., and Wiggert, J. D. (2004). Satellite Evidence of Hurricane-Induced Phytoplankton Blooms in an Oceanic Desert. *J. Geophys. Res.* 109, 1–21. doi: 10.1029/2003JC001938

Chang, J., Chung, C. C., and Gong, G. C. (1996). Influences of Cyclones on Chlorophyll-A Concentration and Synechococcus Abundance in a Subtropical Western Pacific Coastal Ecosystem. *Mar. Ecol. Prog. Ser.* 140, 199–205. doi: 10.3354/meps140199

Chen, C. T. A., Liu, C. T., Chuang, W. S., Yang, Y. J., Shiah, F. K., Tang, T. Y., et al. (2003). Enhanced Buoyancy and Hence Upwelling of Subsurface Kuroshio Waters After a Typhoon in the Southern East China Sea. *J. Mar. Syst.* 42, 65–79. doi: 10.1016/S0924-7963(03)00065-4

Chen, X. Y., Pan, D. L., He, X. Q., Bai, Y., and Wang, D. F. (2012). Upper Ocean Responses to Category 5 Typhoon Megi in the Western North Pacific. *Acta Oceanol. Sin.* 31, 51–58. doi: 10.1007/s13131-012-0175-2

Chen, Y., and Zhao, H. (2021). Spatial Distribution of the Summer Subsurface Chlorophyll Maximum in the North South China Sea. *PLoS One* 16 (4), e0248715. doi: 10.1371/journal.pone.0248715

Cloern, J. E. (1996). Phytoplankton Bloom Dynamics in Coastal Ecosystems: A Review With Some General Lessons From Sustained Investigation of San Francisco Bay, California. *Rev. Geophysics* 34, 127–168. doi: 10.1029/96RG00986

Dou, M., Ma, X. K., Zhang, Y., Zhang, Y. Y., and Shi, Y. S. (2019). Modeling the Interaction of Light and Nutrients as Factors Driving Lake Eutrophication. *Ecol. Model.* 400, 41–52. doi: 10.1016/j.ecolmodel.2019.03.015

Foltz, G. R., Balaguru, K., and Leung, L. R. (2015). A Reassessment of the Integrated Impact of Tropical Cyclones on Surface Chlorophyll in the Western Subtropical North Atlantic. *Geophys. Res. Lett.* 42, 1158–1164. doi: 10.1002/2015GL063222

Fu, D. Y., Pan, D. L., Mao, Z. H., Ding, Y. Z., and Chen, J. Y. (2009). The Effects of Chlorophyll-A and SST in the South China Sea Area by Typhoon Near Last Decade. *Proc. SPIE - International Soc. Optical Eng.* 7478, 74782E–74782E-13. doi: 10.1117/12.830215

Gao, J. S., Wu, G., and Ya, H. Z. (2017). Review of the Circulation in He Beibu Gulf, South China Sea. *Continental Shelf Res.* 138, 106–119. doi: 10.1016/j.csr.2017.02.009

Grobbelaar, J. U. (1990). Modelling Phytoplankton Productivity in Turbid Waters With Small Euphotic to Mixing Depth Ratios. *J. Plankton Res.* 12, 923–931. doi: 10.1093/plankt/12.5.923

Hagy, J. D., Lehrter, J. C., and Murrell, M. C. (2006). Effects of Hurricane Ivan on Water Quality in Pensacola Bay, Florida. *Estuaries nd Coasts.* 29, 919–925. doi: 10.1007/BF02798651

Kaiser, D., Unger, D., and Qiu, G. (2014). Particulate Organic Matter Dynamics in Coastal Systems of the Northern Beibu Gulf. *Continental Shelf Res.* 82, 99–118. doi: 10.1016/j.csr.2014.04.006

Kaiser, D., Unger, D., Qiu, G., Zhou, H., and Gan, H. (2013). Natural and Human Influences on Nutrient Transport Through a Small Subtropical Chinese Estuary. *Sci. Total Environment.* 450-451, 92–107. doi: 10.1016/j.scitotenv.2013.01.096

Kocum, E., Underwood, G., and J.C.and Nedwell, D. B. (2002). Simultaneous Measurement of Phytoplanktonic Primary Production, Nutrient and Light Availability Along a Turbid, Eutrophic UK East Coast Estuary (the Colne Estuary). *Mar. Ecol. Prog. Ser.* 231, 1–12. doi: 10.3354/meps231001

Lai, J. X., Jiang, F. J., Ke, K., Xu, M. B., Lei, F., and Chen, B. (2014). Nutrients Distribution and Trophic Status Assessment in the Northern Beibu Gulf, China. *Chin. J. Oceanology&Limnology.* 2 (5), 1128–1144. doi: 10.1007/s00343-014-3199-y

Lane, R. R., Day, J. W., Marx, B., Reyes, E., and Kemp, G. P. (2002). Seasonal and Spatial Water Quality Changes in the Outflow Lume of the Atchafalaya River, Louisiana, USA. *Estuaries* 25, 30–32. doi: 10.1007/BF02696047

Lao, Q. B., Liu, G. Q., Shen, Y. L., Su, Q. Z., and Lie, X. T. (2021). Biogeochemical Processes and Eutrophication Status of Nutrients in He Northern Beibu Gulf,

South China. *J. Earth System Science volume.* 130, 199. doi: 10.1007/s12040-021-01706-y

Lao, Q. B., Su, Q. Z., Liu, G. Q., Shen, Y. L., Chen, F. J., Lei, X. T., et al. (2019). Spatial Distribution of and Historical Changes in Heavy Metals in the Surface Seawater and Sediments of the Beibu Gulf, China. *Mar. Pollut. Bulletin.* 146, 427–434. doi: 10.1016/j.marpolbul.2019.06.080

Lin, I. I. (2012). Typhoon-Induced Phytoplankton Blooms and Primary Productivity Increase in the Western North Pacific Subtropical Ocean. *J. Geophys. Res. Oceans* 117, C03039. doi: 10.1029/2011JC007626

Lin, I. I., Liu, W. T., Wu, C. C., Wong, G. T., Hu, C., Chen, Z., et al. (2003). New Evidence for Enhanced Ocean Primary Production Triggered by Tropical Cyclone. *Geophys. Res. Letters.* 30 (13), 1718. doi: 10.1029/2003gl017141

Liu, J. L., Cai, S. Q., and Wang, S. G. (2011). Observations of Strong Near-Bottom Current After the Passage of Typhoon Pabuk in the South China Sea. *J. Mar. Syst.* 87 (1), 102–108. doi: 10.1016/j.jmarsys.2011.02.023

Liu, Y. P., Tang, D. L., and Evgeny, M. (2019). Chlorophyll Concentration Response to the Typhoon Wind-Pump Induced Upper Ocean Processes Considering Air-Sea Heat Exchange. *Remote Sens.* 11, 1825. doi: 10.3390/rs11151825

Liu, Y. P., Tang, D. L., Tang, S. L., Morozov, E., Liang, W. Z., and Sui, Y. (2020). A Case Study of Chlorophyll a Response to Tropical Cyclone Wind Pump Considering Kuroshio Invasion and Air-Sea Heat Exchange. *Sci. Total Environ.* 741, 140290. doi: 10.1016/j.scitotenv.2020.140290

Lu, X. Q., Yu, H., Ying, M., Zhao, B., Zhang, S., Lin, L. M., et al. (2021). Western North Pacific Tropical Cyclone Database Created by He China Meteorological Administration. *Adv. Atmospheric Sci.* 38 (4), 690–699. doi: 10.1007/s00376-020-0211-7

Maren, D. S. V. (2007). Water and Sediment Dynamics in the Red River Mouth and Adjacent Coastal Zone. *J. Asian Earth Sci.* 29, 508–522. doi: 10.1016/j.jseaes.2006.03.012

Maren, D. S. V., and Hoekstra, P. (2005). Dispersal of Suspended Sediments in the Turbid and Highly Stratified Red River Plume. *Continental Shelf Res.* 25 (4), 503–519. doi: 10.1016/j.csr.2004.10.010

Maritorena, S., d'Andon, O. H. F., Manginet, A., and Siegel, D. A. (2010). Merged Satellite Ocean Color Data Products Using a Bio-Optical Model: Characteristics, Benefits and Issues. Remote Sens. *Environ.* 114, 1791–1804. doi: 10.1016/j.rse.2010.04.002

Maritorena, S., and Siegel, D. A. (2005). Consistent Merging of Atellite Ocean Color Data Sets Using a Bio-Optical Model. *Remote Sens. Environ.* 94, 429–440. doi: 10.1016/j.rse.2004.08.014

Ma, B., and Zhao, H. (2021). Distribution Characteristics of Chlorophyll-a and Nutrients in the Pearl River Estuary in Summer and Their Relationship With Environmental Factors. *Mar. Environ. Sci.* 40 (05), 707–716. doi: 10.13634/j.cnki.mes.2021.05.008

McKinnon, A. D., Meekan, M. G., Carleton, J. H., Furnas, M. J., Duggan, S., and Skirving, W. (2003). Rapid Changes in Shelf Waters and Pelagic Communities on the Southern Northwest Shelf, Australia, Following a Tropical Cyclone. *Continental Shelf Res.* 23 (1), 93–111. doi: 10.1016/S0278-4343(02)00148-6

Miller, W. D., and Harding, L. W. J. (2007). Climate Forcing of the Pring Bloom in Chesapeake Bay. *Mar. Ecol. Prog. Series.* 31, 11–22. doi: 10.3354/meps331011

Paerl, H. W., Valdes, L. M., Adolf, J. E., and Harding, L. W. J. (2006). Anthropogenic and Climatic Influences on the Eutrophication F Large Estuarine Ecosystems. *Limnol. Oceanogr.* 51, 48–462. doi: 10.4319/lo.2006.51.1_part_2.0448

Price, J. F. (1981). Upper Ocean Response to a Hurricane. *J. Phys. Oceanogr.* 11, 153–175. doi: 10.1175/1520-0485(1981)011<0153:UORTAH>2.0.CO;2

Schaeffer, B. A., Kurtz, J. C., and Hein, M. K. (2012). Phytoplankton community composition in nearshore coastal waters of Louisiana. *Marine Pollution Bulletin.* 64. 1705–1712. doi: 10.1016/j.marpolbul.2012.03.017

Shang, S. L., Li, L., Sun, F. Q., Wu, J. Y., Hu, C. M., Chen, D. W., et al. (2008). Changes of Temperature and Biooptical Properties in He South China Sea in Response to Typhoon Lingling. *Geophys. Res. Lett.* 35 (10), L10602. doi: 10.1029/2008GL033502

Shao, J. C., Zhao, H., Shen, C. Y., and Lv, J. H. (2015). Influence of Typhoon Matsa on Phytoplankton Chlorophyll-A in the Northwest Pactific Ocean Offshore and Alongshore. *J. Guangdong Ocean Univ.* 35 (04), 67–74. doi: 10.3969/j.issn.1673-9159.2015.04.011

Song, H. J., Ji, R. B., and Wang, Z. L. (2011). A Review of Coastal Hytoplankton Bloom Dynamics and Phenology. *Adv. Earth Science.* 26 (3), 257–265. doi: 10.11867/j.issn.1001-166.2011.03.0257

Wang, C. Z., Li, X. H., Qi, J. H., and Su, Y. C. (1998). A Numerical Model for Predicting Offshore SST Anomaly in the East China Sea. *Acta Oceanologica Sinica.* 20 (3), 19–26.

Wetz, M. S., and Paerl, H. W. (2008). Estuarine Phytoplankton Responses to Hurricanes and Tropical Storms With Different Characteristics (Trajectory, Rainfall, Winds). *Estuaries Coasts* 1 (2), 419–429. doi: 10.1007/s12237-008-9034-y

Wu, Z., Jiang, C., Deng, B., Chen, J., Long, Y., Qu, K., et al. (2019). Numerical Investigation of Typhoon Kai-Tak (1213) Using a Mesoscale Coupled WRF-ROMS Model[J]. *Ocean Eng.* 175 (MAR.1), 1–15. doi: 10.1016/j.oceaneng.2019.01.053

Xie, L. L., He, C. F., Li, M. M., Tang, J. L., and Jiang, Z. Y. (2017). Esponse of Sea Surface Temperature to Typhoon Passages Over the Pwelling Zone East of Hainan Island. *Adv. Mar. Science.* 5 (1), 12. doi: 10.3969/j.issn.1671-6647.2017.01.002

Yang, X. X., and Tang, D. L. (2010). Location of Sea Surface Temperature Cooling Induced by Typhoon in the South China Sea. *J. Trop. Oceanogr.* 29 (4), 26–31. doi: 10.1080/09500340.2010.529951

Ying, M., Zhang, W., Yu, H., Lu, X. Q., Feng, J. X., Fan, Y. X., et al. (2014). An Overview of the China Meteorological Administration Opical Cyclone Database. *J. Atmospheric Oceanic Technol.* 31, 287–301. doi: 10.1175/JTECH-D-12-00119.1

Zhang, Y. L., Qin, B. Q., and Chen, W. M. (2003). Advances and Ain Applications of Lake Optics Research. *Adv. Water Sci.* (05), 653–659. doi: 10.3321/j.issn:1001-6791.2003.05.023

Zhao, H., Han, G. Q., Zhang, S. W., and Wang, D. X. (2013). Two Hytoplankton Blooms Near Luzon Strait Generated by Lingering Yphoon Parma. *J. Geophys. Research: Biogeosciences.* 18 (2), 412–421. doi: 10.1002/jgrg.20041

Zhao, H., Pan, J. Y., Han, G. Q., Devlin, A. T., Zhang, S. W., and Hou, Y. (2017). Effect of a Fast-Moving Tropical Storm Washi on Phytoplankton in the Northwestern South China Sea. *J. Geophys. Research: Oceans* 122, 3404–3416. doi: 10.1002/2016JC012286

Zhao, H., Tang, D. L., and Wang, Y. Q. (2008). Comparison of Hytoplankton Blooms Triggered by Two Typhoons With Different Ntensities and Translation Speeds in the South China Sea. *Mar. Ecology Prog. Series.* 365, 57–65. doi: 10.3354/meps07488

Zhao, H., Tang, D. L., and Wang, D. X. (2009). Phytoplankton Looms Near the Pearl River Estuary Induced by Typhoon Nuri. *J. Geophys. Res.* 114, C12027. doi: 10.1029/2009JC005384

Zhao, H., and Zhang, S. P. (2014). Review on Spatial-Temporal Ariation of China' Offshore Phytoplankton Chlorophyll and Primary Roductivity and Their Variational Mechanism. *J. Guangdong Ocean Univ.* 34, 98–104. doi: 10.3969/j.issn.1673-159.01.016

Zheng, G. M., and Tang, D. L. (2007). Offshore and Nearshore Chlorophyll Increases Induced by Typhoon Winds and Subsequent Terrestrial Rainwater Runoff. *Mar. Ecol. Prog. Series.* 333, 61–74. doi: 10.3354/meps333061

Conflict of Interest: The authors declare that the research was conducted in the absence of any commercial or financial relationships that could be construed as a potential conflict of interest.

Publisher's Note: All claims expressed in this article are solely those of the authors and do not necessarily represent those of their affiliated organizations, or those of the publisher, the editors and the reviewers. Any product that may be evaluated in this article, or claim that may be made by its manufacturer, is not guaranteed or endorsed by the publisher.